237D Fusion Technology
Handout v. 9.2

Professor Mohamed Abdou

February 9, 2016

Chapter 1

Radiation Shielding

1.1 Page 1

1.2 Page 2

1.2.1 Types of Shielding in Fusion Reactor

- bulk shield (surrounding the blanket to protect vacuum vessel and superconducting magnets.
- Penetration shield (around penetrations, e.g. natural beams, vacuum ducts)
- Biological (reactor building walls, typically concrete; protect personnel in central rooms and outside.)

1.3 Page 3

1.3.1 Bulk Shield

This is a large component of fusion reactor. It is outside the blanket and inside the vacuum vessel. Topics to be covered

- Shield material composition
- Radiation damage to superconducting magnet materials
- Optimization of inboard blanket/shield thickness

1.4 Page 4

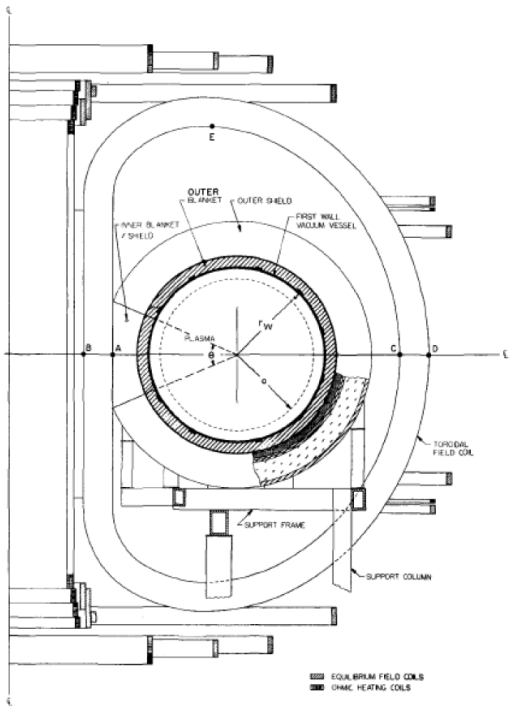

Fig. 4. A simplified vertical cross section of a representative tokamak with circular plasma.

Figure 1.1: A simplified vertical cross section of a representative tokamak with circular plasma.

1.5 Page 5

1.5.1 Shield Composition

A considerable fraction of the neutrons leaking from the blanket have kinetic energies above a few MeV. A basic requirement therefore of the shielding material is to have a large attenuation coefficient for high energy neutrons. Inevitably, this has to be a material of moderate of large mass number since inelastic scattering is the most efficient mechanism for reducing the energies of high energy neutrons. Furthermore, light materials such as water, LiH, and lithium have small total cross sections at high energies when compared with heavy materials. Stainless steel and lead have relatively large total cross sections above 3 MeV and the average secondary neutron energy per inelastic collision at 14 MeV is 2.2 and 2.5 MeV in lead and iron, respectively. Both materials are available, relatively inexpensive, and a great deal of knowledge about their characteristics exist. Below the

inelastic threshold, however, these materials are no longer effective and a light material should be present. Borated water is efficient and is almost cost free. However, the presence of water in the same system with a high-temperature liquid metal increases significantly the hazard of accidental energy release. Graphite is an alternative choice. In addition, to minimize the gamma emission from radiative capture reactions, it is essential to use a sufficient amount of B^10 which has a large (n,α) cross section for low energy neutrons and is associated with only soft gamma (0.5 MeV) emission (compared with a strong line at 7.6 MeV in the capture gamma ray spectrum for iron). Boron carbide B_4C irradiation but helium production is large. However, if B_4C is used in the shield with only 80% of the theoretical density, the swelling problem due to the excessive helium production can be tolerated. Boral (50% B_4C and 50% Al) is another good choice.

Based on the above discussion, a mixture of stainless steel and boron carbide, or of lead and B_4C, or a combination of the three materials are reasonable choices and further investigation is needed to find the optimum composition and shield depth for an overall low cost. For this purpose, a fixed composition and configuration of the blanket coupled to a shield for which the parameters are to be varied as shown in figure FIGURE is considered. The blanket consists of a 1 cm first wall, 42 cm of 95% Li plus 5% structure. The first wall and blanket structure is niobium in the following calculations but the results in the shield are insensitive to this choice. The extra 7 m of lithium at the outer face of the reflector region was introduced to meet the cooling requirements of the reflector and inner regions of the shield. As preliminary criteria, the attenuation required in the blanket and shield should be roughly 10^6. This requirement can be satisfied by approximately 70 cm of stainless steel plus boron carbde following the blanket described above. As a starting point, figure FIGURE in which the blanket is followed by a one meter shield was considered as a reference design for investigating various aspects of the shield design. Six cases for the composition of the shield were considered; 70% SS plus 30% B_4C (design 114), 70% Pb plus 30% B_4C (design 115), 35% SS plus 35% Pb plus 30% B_4C (design 115), 100% SS (design 117), 85% Pb + 15% B_4 (design 118), and 50%, where percentages are by volume. Neutronics and photonics calculations were carried out for the six designs. It has been shown REFERENCE that the convergence of the discrete ordinates results for such a system are achieved by S_8 and S_4 overestimates the leakage by 10 to 15%. In order to reduce the cost for these calculations, S_4 was used. The comparison is not significantly affected by the difference between S_4 and S_8. Cylindrical geometry and the P_3 approximation of the scattering anisotropy were used in all calculations.

The energy leakage, L_{TE}, is plotted against the distance from the inner boundary of the shield for designs 114 through 117 in fig. FIGURE and for designs

1.6 Page 6

115, 118, and 119 in figure FIGURE. L_{TE}, is the sum of the neutron energy leakage, L_{nE}, and the gamma energy leakage, $L_{\gamma E}$, where L_{nE} is defined in the multigroup representation at any surface of a one-dimensional cylinder as

$$L_{nE}(r) = 2\pi r \sum_g E_{ng}(r) J_{ng}(r) \tag{1.1}$$

Where J_{ng} is the (net) neutron current density at the surface in energy group g, and E_{ng} is approximated by the midpoint energy of group g. Similar definitions apply for gammas with the subscript γ replacing n. Since the energy deposition in the magnet by neutrons and photons streaming out of the shield increasing, in general, with the neutron and photon energies we find it more meaningful in comparing the performance of various shield compositions to compare the "energy" rather than the "number" attenuations. The results in figures FIGURES show that L_{TE} varies exponentially with the spatial variable, r, i.e.

$$L_{TE}(r) = L_{TE}(r_0) e^{-\mu_t (r - t_0)} \tag{1.2}$$

Where μ_t (with or without the subscript) is the total energy attenuation coefficient. Similar results were found for both the neutron and gamma fluxes i.e.

$$L_{nE}(r) = L_{nE}(r_0) e^{-\mu_n (r - t_0)} \tag{1.3}$$

$$L_{\gamma E}(r) = L_{\gamma E}(r_0) e^{-\mu_\gamma (r - t_0)} \tag{1.4}$$

The energy attenuation coefficients μ_n, μ_γ, and μ_t obtained for the six designs discussed above are given in table TABLE. Several conclusions can be reached from examining the attenuation curves of figures FIGURES and the energy attenuation coefficients in table TABLES: 1- Comparison of L_{TE} for designs 114, 115 and 116 shows that stainless steel has considerably better attenuation characteristics than lead if both are mied with a fair amount of light material. 2- Comparison of L_{TE} for designs 114 and 117 shows that the presence of B_4C (or an alternative) is necessary. At the end of a one meter shield the total energy leakage from a 100% stainless steel shield is about two orders of magnitude higher than that from a shield consisting of 70% SS plus 30% B_4C. This is mainly due to two causes. B_4C is better than SS at attenuating neutrons below about 2 MeV. In addition, in the absence of B^{10}, neutrons slowed down eventually get absorbed in radiative capture reactions in stainless steel increasing the gamma energy production. 3- Figure FIGURE which compares L_{TE} for 85% Pb + 15% B_4C, 70% Pb + 30% B_4C, and 50% Pb + 50% B_4C shows that increasing the volume percentage of B_4C to 50% (and probably higher) improves the attenuation considerably. If other light materials such as graphite or water are used, the optimal volume percentages are usually much less (roughly 30%)

than that for B_4C. 4- Although lead is more efficient in attenuating gamma radiation, we found that using stainless steel does not increase the gamma energy leakage, $L_{\gamma E}$, appreciably. Furthermore, table TABLE shows that μ_γ is greater in stainless steel-B_4C than in Pb-B_4C mixtures. These results can be explained as follows. The photons in the shield come primarily from gammas produced by neutron interactions in the shield rather than by penetration from the blanket. Stainless steel attenuates fast neutrons quickly in the first few mean free paths, thus the photons produced have a long distance in which to be absorbed. In addition, the gamma energy leakage in the outer regions is affected most by the gammas produced in these regions. The seconday gama production in deeper regions of a SS-B_4C shield is significantly lower than in the same regions of the Pb-B_4C shield.

1.6.1 Optimization of a Shield Thickness

Increasing the thickness of a shield increases its cost and the magnet

1.7 Page 7

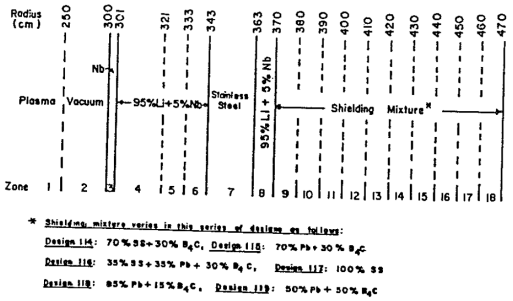

Fig. 1. Reference design for shield calculations

Figure 1.2: Reference design for shield calculations.

Design ID	114	115	116	117	118	119
Shield Composition (all percentages are by volume)	70% SS + 30% B_4C	70% Pb + 30% B_4C	35% Pb + 35% SS + 30% B_4C	100% SS	85% Pb + 15% B_4C	50% Pb + 50% B_4C
Neutron Energy Attenuatuion Coefficient, μ_n (cm^{-1})	0.1438	0.1113	0.1282	0.1022	0.0977	0.1161
Gamma Energy Attenuation Coefficient, μ_γ (cm^{-1})	0.1466	0.1160	0.1320	0.0828	0.1008	0.1190
Total Energy Attenuation Coefficient, μ_t (cm^{-1})	0.1445	0.1113	0.1283	0.0902	0.0976	0.1161

Table 1.1: Neutron, Carma, and Total Energy Attenuation Coefficients* for Various Shield Compositions

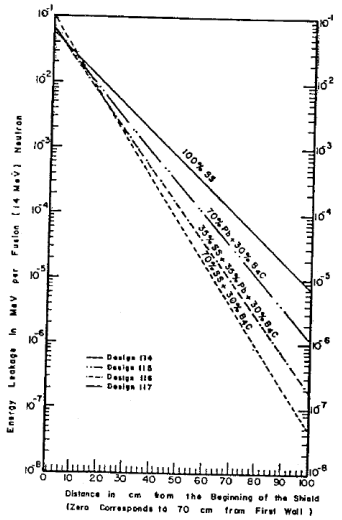

Fig. 2. Energy leakage versus depth in various shield compositions

Figure 1.3: Energy leakage versus depth in various shield compositions.

1.8 Page 8

* obtained by fitting the energy attenuation curves to exponentials (see Text)

1.9 Page 9

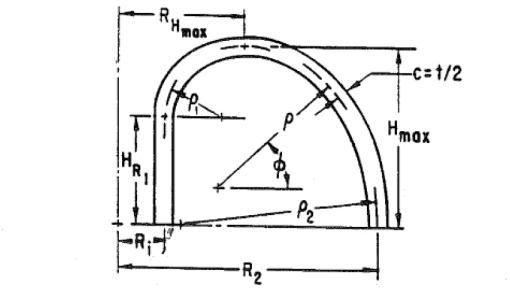

Figure 3. Geometric Parameters for a Constant-Tension Coil

Figure 1.4: Geometric Parameters for a Constant *** I DON'T KNOW THIS WORD***.

1.10 Page 10

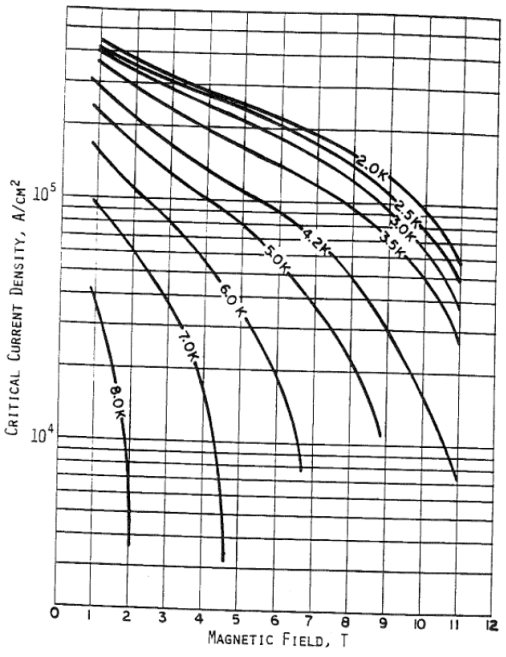

Figure 2. J-H Curve for NbTi Versus Temperature

Figure 1.5: J-H Curve for NbTi Versus Temperature.

1.11 Page 11,12,13

These pages were already in handout 9.

1.12 Page 14

1.12.1 Optimization of Inboard Blanket and Shield Thickness in Tokamak

Tradeoffs between:

- Reactor size, reactor power, magnetic field, etc.
- Protection of S.C. Magnet

1.13 Page 15

1.13.1 Motives for Larger Blanket and Shield Thickness

Shield Function: Radiation protextion of S.C. magnet

$$\phi_m \sim \phi_w e^{-\mu \Delta_{BS}^i} \tag{1.5}$$

ϕ_w = flux at first wall (fixed by design)μ = attenuation coefficient (fixed by shielding composition) (1.6)

Magnet Protection

- Refrigeration power requirements
- Change in superconductor J_c, T_c
- Radiation-induced resistivity in stabilizer
- Change in mechanical and dielectric properties of insulators

1.14 Page 16

1.14.1 Motive for Smaller Blanket / Shield Thickness